8th International Conference on CFD in Oil & Gas, Metallurgical and Process Industries
SINTEF/NTNU, Trondheim Norway *CFD11-124*
21-23 June 2011

PARCEL-BASED APPROACH FOR THE SIMULATION OF GAS-PARTICLE FLOWS

Stefan RADL[1]*, Charles RADEKE[2], Johannes G. KHINAST[2,3], Sankaran SUNDARESAN[1]

[1]Department of Chemical and Biological Engineering, Princeton University, Princeton, NJ

[2]Research Center Pharmaceutical Engineering GmbH, Graz, Austria

[3]Institute for Process and Particle Engineering, Graz University of Technology, Graz, Austria

* E-mail: sradl@princeton.edu

ABSTRACT

We focus on a parcel-based approach, similar to the one used by O'Rourke and Snider, 2010, which tracks the motion of a so-called "parcel" of particles. We derive a scaling law for a linear-spring dashpot interaction model that enables tracking of clouds of particles through DEM-based simulation of (scaled) pseudo-particles. This guarantees convergence to a DEM-based simulation of the unscaled system, i.e., a system where all the individual particles are tracked. We use a BGK-like relaxation term to model collisions between particles in dilute regions of the flow field. This combined approach is implemented in an in-house code that runs on GPUs (Radeke et al., 2010), and is used to study a granular jet impinging on a plane surface, as well as a simple shear flow. We find that a BGK-type relaxation model is necessary when using parcel-based approaches for capturing some prominent flow features.

Keywords: Discrete element method, simulation, granular impinging jet, shear flow.

NOMENCLATURE

Latin Symbols

c	Damping coefficient of primary particles, [kg/s].
C	Constant in the filter function.
d	Diameter, [m].
e_p	Coefficient of restitution.
E	Young's modulus, [N/m²].
f	Particle distribution function.
$\mathbf{F}$	Force, [N].
g_0	Radial distribution function.
G	Filter function.
h	Switch-off function.
k	Stiffness of primary particles, [N/m].
K	Constant.
m	Mass, [kg].
N	Number of particles in a parcel.
p	Pressure, [N/m²].
P	Probability distribution function.
R	Radius, [m].
r_{32}	Sauter mean radius of primary particles, [m].
t	Time, [s].
T	Granular temperature, [m²/s²].
$\mathbf{T}$	Torque, [N·m].
U	Initial velocity, [m/s].
$\mathbf{v}$	Velocity, [m/s].
y	Vertical distance, [m].

Greek Symbols

α	Scaling ratio.
β	Size ratio of colliding particles.
δ	Overlap, [m].
Δ	Dimensionless filter length.
ϕ	Volume fraction.
γ	Shear rate, [1/s].
η	Damping function.
κ	Exponent.
λ	Experimental parameter for the scattering angle.
μ	Friction coefficient.
Π	Dimensionless parameter.
θ	Scattering angle, [rad].
ρ	Particle density, [kg/m³].
$\boldsymbol{\sigma}$	Stress, [N/m²].
τ	Shear stress [N/m²].
τ_D	Relaxation time, [s].
$\boldsymbol{\omega}$	Rotation rate, [rad/s].

Sub/superscripts

*, *'	Dimensionless quantities.
BGK	Bhatnagar–Gross–Krook.
CP	Close packed.
eff	Effective.
el	Elastic.
eq	Equilibrium.
fluct	Fluctuation.
half	Half.
impact	At impact.
jet	Jet.
model	Modeled term.
n	Normal direction.
t	Tangential direction.
off	Value at switch-off.
p	Parcel.
prim	Primary particle.

PP	Particle-particle.
PW	Particle-wall.
roll	Rolling.
sample	At sample position.
0	Reference value.

INTRODUCTION

Discrete Particle Models (DPM), aim at tracking individual particles, or parcels thereof, in the flow domain. By using this approach, the treatment of a granular assembly made up by particles with different, size, density, shape, or composition is straightforward. Particle-based methods offer the possibility to include complex particle-wall interactions, the handling of rare events, as well as to extend the method to gas-particle-droplet systems (Link et al., 2009; O'Rourke et al., 2009; Zhao et al., 2009). Interest in the latter systems has been recently motivated by the pharmaceutics industry (Radeke and Khinast, 2011; Radeke et al., 2010), and also by classical applications like coking (typically performed in fluidized beds, see Darabi et al., 2010; Radmanesh et al., 2008), or catalyst impregnation.
When using a DPM, two major approaches can be chosen: First, each particle in the system can be tracked. In this case, relatively simple models based on instantaneous ("hard-sphere" model), or enduring collision dynamics ("soft-sphere" model, recently summarized by Cleary, 2009) can be employed. The soft-sphere approach is more general, and allows also for the simulation of dense regions with enduring contacts, and is usually referred to as "Discrete Element Method" (DEM).
Second, the particle population can be represented by so-called "parcels" of particles, i.e., a cloud of particles, and hence the name parcel-based approach. Another way of interpreting such an approach is to think of a (discrete) approximation of the particle distribution function by test particles. For gas-solid flows, Andrews and O'Rourke, 1996, proposed the so-called "Multi-Phase Particle-In-Cell" (MP-PIC) approach, which is a parcel-approach. MP-PIC has been applied widely to fluidized beds, sedimentation, hopper flow, as well as other dense granular flows (O'Rourke et al., 2009; O'Rourke and Snider, 2010; Snider, 2001; Snider, 2007). In principle, a parcel-based approach does not require a second-phase to be present; however, MP-PIC requires an implicit coupling to the fluid phase due to stability reasons. The MP-PIC approach does not track collisions between particles directly, but employs a simple "particle pressure" model to prevent particles from becoming close-packed. Instead of modeling particle interaction forces with a particle pressure, Patankar and Joseph, 2001, explored the use of a simple soft-sphere model (without friction) in conjunction with a parcel-based method for a relatively small system. A similar approach was taken by Sakai et al., 2010; Sakai and Koshizuka, 2009, as well as Mokhtar et al., 2011.
Only recently Bierwisch et al., 2009 have shown that a parcel-based approach with contact detection, when using appropriately scaled interaction parameters, yields simulation results independent of the number of particles making up the parcel. Bierwisch et al., 2009 showed that this scaling must be based on identical (i) particle density, (ii) coefficient of restitution, (iii) friction coefficients, and (iv) Young's modulus for their Hertzian repulsion force model. The scaling proposed by Bierwisch et al., 2009 yields stresses in the quasi-static regime, and parcel velocities in all regimes, that are scale independent. However, the analysis of Bierwisch et al., 2009, is based on a single collision, and studies on parcel behavior in dense to moderately dense systems (i.e., for particle volume fractions between 0.05 and 0.50) are still lacking.
Our first objective is to provide a scaling for the parameters of a DEM-based (linear spring-dashpot) model, such that stresses and velocities in the quasi-static flow regime are scale independent. Our second objective is to establish a method that takes the effect of sub-parcel collisions, not directly tracked when using a parcel-based approach, into account. We base our method on the ideas of O'Rourke and Snider, 2010. However, we aim at a strategy that is consistent with DEM, i.e., that yields a "pure" DEM-based simulation in a situation where only one particle is in the parcel. Our third objective is to demonstrate the effect of the proposed scaling and the sub-parcel collision model on the dynamics of two granular flows. Our simulations are based on an in-house code running on graphic processing units (GPUs).

MODEL DESCRIPTION

Dense Region

When using a parcel-based approach, one has to prevent over-packing in dense regions either with an (indirect) particle pressure model (Andrews and O'Rourke, 1996), or a model based on the direct detection of particle collisions (e.g., the strategy followed by Patankar and Joseph, 2001). In our model we have chosen to account for collisions by using a linear spring-dashpot model (see Eqns. 1-2), which is well established for granular dynamics. The details of our implementation are provided in Radeke et al., 2010, and here we only provide the most essential model equations. For our present work we included a spring-dashpot-slider model in the tangential direction (see Eqn. 2), as well as a rolling friction model between particles, and particles and the wall (see Eqns. 3-5; $\mathbf{v}_{roll}$ is a "rolling velocity" as defined by Luding, 2008).

$$\mathbf{F}_{ij,n} = k_n \cdot \delta_n \cdot \mathbf{n} + c_n \cdot \dot{\delta}_n \cdot \mathbf{n} \tag{1}$$

$$\mathbf{F}_{ij,t} = \min\left(\mathbf{F}_{ij,n} \cdot \mu,\ k_t \cdot \delta_t \cdot \mathbf{t} + c_t \cdot \dot{\delta}_t \cdot \mathbf{t}\right) \tag{2}$$

$$\mathbf{F}_{roll} = -\mu_{roll} \cdot \mathbf{F}_n \cdot \mathbf{v}_{roll} \big/ \left|\mathbf{v}_{roll}\right| \tag{3}$$

$$\mathbf{v}_{roll} = -R_{eff} \cdot \left[\mathbf{n} \times \boldsymbol{\omega}_1 - \mathbf{n} \times \boldsymbol{\omega}_2\right] \tag{4}$$

$$\mathbf{T}_{roll} = R_1 \cdot \mathbf{n} \times \mathbf{F}_{roll} \tag{5}$$

The central question when using a DEM-based model for the parcel-based approach is how to connect particle interaction parameters with parcel interaction parameters. Specifically, we ask the question, how

spring stiffness and damping coefficient must be scaled, when a parcel with a diameter $d_p = \alpha \cdot d_{prim}$ is used in the simulation (α is the ratio of the parcel diameter to the primary particle diameter).
In the following we describe the details on such a scaling that yields identical stresses for dense granular flow using the linear spring-dashpot model (Eqns. 1-5).

Scaling of Interaction Parameters

We base our analysis on equal energy densities in the original, and the coarse-grained system. This means that the density of the particles, as well as the translational velocity must be invariant. Also, the total rotational kinetic energy of the original and coarse-grained particles must be identical. The following analysis is valid for a linear spring-dashpot model with frictional slider, and is similar to the analysis for a Hertzian interaction model by Bierwisch et al., 2009. Since we base our analysis on an effective mass and radius for the collision, it is valid for both particle-wall, as well as for particle-particle collisions with arbitrary size ratios of the primary particles (i.e., the particles in the original system). Our analysis does not include differences in particle densities; however, an extension to these systems can be easily done in analogy to particle size differences.
We start with the differential equation for the overlap in normal direction from Newton's equation of motion:

$$m_{eff} \cdot \ddot{\delta}_n = k_n \cdot \delta_n + c_n \cdot \dot{\delta}_n . \tag{6}$$

Here the effective mass is:

$$m_{eff} = \frac{m_i \cdot m_j}{(m_i + m_j)} = \frac{4\pi}{3} \frac{R_i^3 \cdot \rho_p \cdot \beta^3}{1+\beta^3} . \tag{7}$$

The effective radius is

$$R_{eff} = \frac{R_i \cdot R_j}{(R_i + R_j)} = \frac{R_i \cdot \beta}{1+\beta} . \tag{8}$$

Inserting these expressions, and using the dimensionless variables $\delta_n{*} = \delta_n / R_i$, $\dot{\delta}_n{*} = \dot{\delta}_n / v_0$, and $t{*} = t/(R_i/v_0)$, as well as approximating Young's modulus with $E \approx k_n / R_i$ yields:

$$K_1 \cdot \ddot{\delta}_n{*} = \frac{k_n \cdot \delta_n{*}}{R_i \cdot \rho_p \cdot {v_0}^2} + \frac{c_n}{R_i^2 \cdot \rho_p \cdot v_0} \cdot \dot{\delta}_n{*} , \tag{9}$$

with $K_1 = 4\pi \cdot \beta^3 / [3(1+\beta^3)]$. Thus, our scaling is based on the dimensionless (normal) overlap for the translational motion of a particle, with the reference length being the parcel diameter in the parcel approach and the particle diameter in the original unscaled problem, i.e., the relative overlap will remain invariant when scaling the system. From Eqn. 9 the following dimensionless parameters can be identified:

$$\Pi_1 = \beta , \; \Pi_2 = k_n / (R_i \cdot \rho_p \cdot {v_0}^2), \quad \Pi_3 = c_n / (R_i^2 \cdot \rho_p \cdot v_0) \tag{10}$$

Π_1 requires a constant ratio of the radii of the colliding particles or parcels. This ratio will remain constant, as long as each parcel is made up by the same number of particles N. Π_2 requires that $k_n / R_i = const$, since we require also the density and the reference velocity v_0 to be invariant. This is in agreement with the simulation results of Chialvo et al., 2010, which found that the pressure scales with k_n / R in a monodisperse, quasi-static granular flow.
Also, the stresses will be identical during scaling. This is because the ratio of the elastic normal forces in the original and scaled system is given by $F_{ij,n}{}^{el'} / F_{ij,n}{}^{el} = (k_n \cdot \alpha) \cdot (\delta_n{*} \cdot \alpha \cdot R_i) / [k_n \cdot \delta_n{*} \cdot R_i] = \alpha^2$.
(our analysis was based on invariant non-dimensional overlaps $\delta_n{*}$). Since the macroscopic contact stress is given by the sum of the dyadic product of contact forces and the distances between two particles in a control volume (see Latzel et al., 2000, for details on the evaluation of stress tensors), the stresses are invariant when using this scaling in the dense regime.
Π_3 requires that $c_n / {R_i}^2 = const$, i.e., c_n scales with α^2, which results in an invariant coefficient of restitution when scaling the system, as well as a damping force that scales with α^2. Finally, it is easy to see that the already dimensionless friction coefficients μ and μ_{roll} must be kept constant when scaling the system.

Dilute Region

Previous Work

To take collisional effects between the particles in a parcel into account, O'Rourke and Snider, 2010, proposed a relaxation of the particle distribution function f to an equilibrium distribution f_{eq} in a BGK-like fashion (in our discrete approximation, f is represented by parcels having individual velocities $\mathbf{v}$). Thus, they set:

$$\frac{\partial f}{\partial t} = \frac{f_{eq} - f}{\tau_D} \tag{11}$$

to take into account particle collisions. O'Rourke and Snider, 2010, suggested the following correction to the parcel velocity to take collisions of particles within the parcel into account:

$$\mathbf{v}' = \frac{\mathbf{v} + (\delta t / (2\tau_D)) \cdot \bar{\mathbf{v}}}{1 + (\delta t / (2\tau_D))} \tag{12}$$

Here, δt is the computational time step, and the mass-averaged particle velocity $\bar{\mathbf{v}}$ is given by a summation over parcels p near the parcel under consideration:

$$\bar{\mathbf{v}} = \sum_p (N \cdot m_{prim} \cdot \mathbf{v}) \Big/ \sum_p (N \cdot m_{prim}) , \tag{13}$$

where m_{prim} is the mass of primary particles, and N is the number of particles in each parcel. O'Rourke and Snider, 2010, proposed Eqns. 14 to 16 for calculating the damping time τ_D.

$$g_0(\phi_p) = \frac{\phi_{p,CP}}{\phi_{p,CP} - \phi_p + eps} \tag{14}$$

$$\eta = (1 + e_p)/2 \tag{15}$$

$$\frac{1}{\tau_D} = \frac{8\cdot\sqrt{2}}{3\cdot\pi}\cdot\frac{\phi_p}{r_{32}^3}\cdot g_0\left(\phi_p\right)\cdot\eta\cdot\left(1-\eta\right)\cdot \frac{\sum_p N\cdot\left(d_{prim}/2+r_{32}\right)^4\cdot\left(\mathbf{v}-\overline{\mathbf{v}}\right)^2}{\sum_p N\cdot\left(d_{prim}/2+r_{32}\right)^2\cdot\sqrt{\left(\mathbf{v}-\overline{\mathbf{v}}\right)^2}} \quad (16)$$

Here *eps* is a small number (taken to be 10^{-5}), r_{32} is the local Sauter-mean radius, and d_{prim} is the (primary) particle diameter of the particles making up the parcel. Eqn. 16 is based on the kinetic theory of granular flow with corrections for particle inelasticity, as well as local particle volume fraction. Also, one can take frictional contacts between particles into account by using an effective coefficient of restitution as proposed by Jenkins and Berzi, 2010. However, it should be kept in mind that the velocity relaxation proposed by O'Rourke and Snider, 2010, applies for an approach where collisions between parcels are not detected; when such collisions are detected, as in our present study, one must modify Eqn. 16 to avoid overdamping.

Modified Relaxation Model for Parcel Velocities

The equation for the collision frequency proposed by O'Rourke and Snider, 2010, models the effect of collisions between particles in different parcels. However, since we are already accounting for collisions between parcels in our implementation (via the spring-dashpot model), we need to model only collisions that occur with a frequency $1/\tau_{D,model}$, i.e.,

$$1/\tau_{\mathrm{D,model}} = 1/\tau_{\mathrm{D}} - 1/\tau_{\mathrm{D,p}} . \quad (17)$$

Assuming that the latter collision frequency between parcels follows the expression in Eqn. 16, and by requiring that the fluctuation velocities of particles and parcels are identical, one obtains:

$$1/\tau_{\mathrm{D,model}} = 1/\tau_{\mathrm{D}}\left(1-1/\alpha\right) . \quad (18)$$

Hence, the frequency of collisions $1/\tau_{D,model}$ that requires modeling in addition to the "resolved" collisions of the parcels, is somewhat lower in our model than the one proposed by O'Rourke and Snider, 2010. Note, that Eqn. 18 is consistent with a "full" simulation of the original system, where all particles are tracked, i.e., $\alpha = 1$ and $1/\tau_{D,model}$ equals zero.

Furthermore, we have to consider a correction in the dense limit, where parcel-parcel collisions become more frequent, and Eqn. 16 is no longer valid. This is because in the limit of close packing, contact forces due to enduring contacts (calculated directly with the spring-dashpot model) will already lead to a velocity relaxation. Thus, we have to reduce the modeled collision frequency at a certain volume fraction $\phi_{p,off}$ to avoid the divergence of $1/\tau_{D,model}$ at $\phi_p = \phi_{p,CP}$. We do this by multiplying Eqn. 18 with a factor $h(\phi_p)$ that approaches zero when ϕ_p equals $\phi_{p,CP}$:

$$h\left(\phi_p\right) = \min\left(1, \left[\frac{\phi_{p,CP}-\phi_p}{\phi_{p,CP}-\phi_{p,off}}\right]^{\kappa_{off}}\right) . \quad (19)$$

Here κ_{off} is an exponent that controls how fast the collision frequency model is switched off. We choose κ_{off} to be 8 for a rapid switch off, and $\phi_{p,off}$ = 0.60. This rather abrupt switch off is motivated by the publications of Silbert et al., 2007, Reddy and Kumaran, 2007, as well as Chialvo et al., 2011. These authors show that there is an abrupt switch between an inertial regime (where the model given by Eqns. 14 and 18 is appropriate) and a quasi-static regime, for which a more complex rheological model has to be used (in our case the DEM-based model shown in Eqns. 1-5).

In summary, our modified relaxation model is consistent with a DEM-based simulation in the dense regime, and with a "full" DEM-based simulation in case the original system is modeled, i.e., a situation where α equals 1. In the dilute limit, and when the parcel size is much larger than the particle size, our relaxation model is identical to the model based on kinetic theory shown in O'Rourke and Snider, 2010.

Local Particle Volume Fraction and Velocity

For the relaxation of parcel velocities, one needs to know the local mean particle volume fraction ϕ_p, as well as the mean velocity of the parcels $\overline{\mathbf{v}}$. Previous work (e.g., O'Rourke and Snider, 2010) used a Cartesian grid for this purpose. This requires an interpolation of particle volume and velocity from and to this grid. We, however, reconstruct ϕ_p and $\overline{\mathbf{v}}$ from a spatial filtering on a spherical domain surrounding each parcel. Our filter function has the form:

$$G(R) = \begin{cases} C_2 + \left(R_0/R\right)^2 & R < \left(R_i + R_j\right)\cdot\Delta_{BGK} \\ 0 & R \geq \left(R_i + R_j\right)\cdot\Delta_{BGK} \end{cases} , \quad (20)$$

with parameters C_2, and R_0 chosen such that the integral of $G(R)$ in a spherical domain is unity. This filter guarantees that the mean quantities are evaluated at the center of the parcel. For our simulations we choose Δ_{BGK} = 3, i.e., filtering was performed in a sphere with a diameter three times the parcel diameter.

RESULTS

Granular Jet

Cheng et al., 2007, have experimentally investigated the normal impact of 0.050 mm to 2.1 mm glass and brass particles (monodispers and spherical) on a circular disc. They showed that the characteristic scattering angle θ_{half} of the rebounding particles is influenced by the ratio of particle and jet diameter d_p/d_{jet}:

$$\theta_{half} = \mathrm{atan}\left(\lambda\cdot 2\cdot d_p/d_{jet}\right) \quad (21)$$

with λ = 1.05 ± 0.05. Thus, for a small particle-to-jet ratio the granular jet behaves like a liquid without a scattering of particle velocities. When using our parcel-approach, the goal is that only the size of the primary particles should affect the scattering angle, and not the parcel diameter itself.

We performed simulations using (i) an unscaled system (i.e., the interaction parameters in Eqns. 1-5 were not

changed with parcel size); (ii) a scaled system (scaling based on the dimensionless parameters displayed in Eqn. 10), but without relaxation model; as well as (iii) a scaled system with the relaxation model shown in Eqn. 18. Also, a simulation of the original system, for which the motion of the primary particles was calculated directly, was performed. The simulation parameters are listed in Table 1. The damping coefficient c_n was calculated from the coefficient of restitution (see Luding, 2008), and we set $c_t = c_n$.

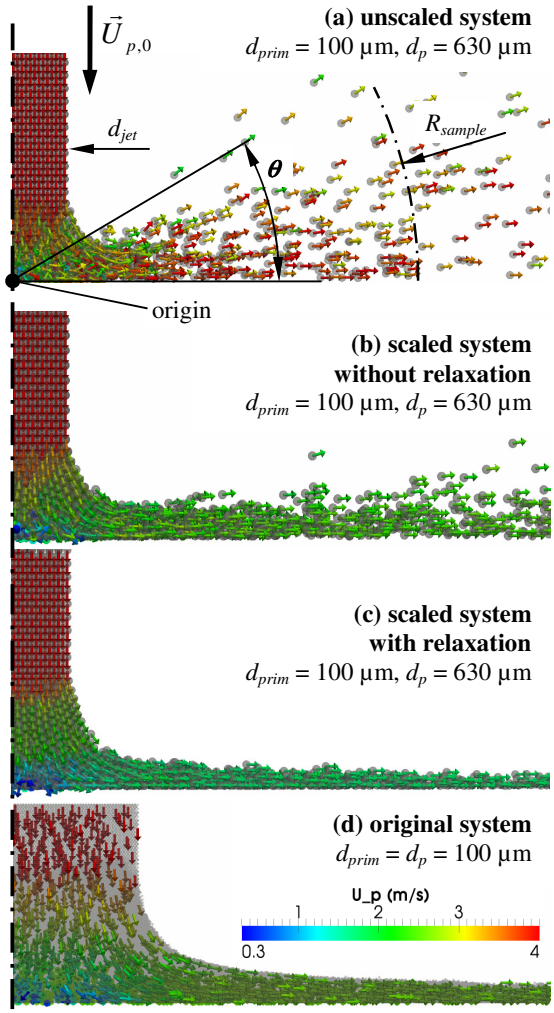

Figure 1: Particle velocities near the impact region of a granular jet. The jet (which has a circular cross section with diameter d_{jet}) impacts the planar surface under an angle of $\theta_{impact} = \pi/2$.

The scattering patterns of these three systems are shown in Figure 1a-c; a magnified version of a slightly smaller region near the impact point for the original system is shown in Figure 1d. Here we show front views of the particle jet, which approaches the planar surface from the top. For the results displayed in Figure 1 we have chosen the scaling factor α as 6.3, i.e., we have grouped 250 single particles into one parcel.

As can be easily seen from Figure 1a, the unscaled system represents a case with a much larger (effective) particle diameter, and the characteristic scattering angle is much larger than that observed in the original system (see Figure 1d). This behavior is expected, since we do not perform any scaling, and the scattering angle is in good agreement with the experimental results of Cheng et al., 2007 (see the comparison of simulation results for the unscaled system indicated by dots with the correlation indicated by the bold line in Figure 3).

Table 1: Parameters for the granular jet simulations.

Parameter	*Value*
d_{jet}	7.3 [mm]
y_{jet}	25 [mm]
d_{jet} / d_p	3.5; 14.6; 29.2; 73
d_p	0.10 - 2.19 [mm]
$U_{p,0}$	1 - 8 [m/s]
ϕ_p	0.60
ρ_p	2500 (glass)
e_p	0.75, 0.95
μ_{PP}	0.10
μ_{PW}	0.15
μ_{roll}	0.01
k_n	306 [N/m]
k_t	88 [N/m]
R_{sample}	63.5 [mm], 20 [mm]

Appropriate scaling of the system significantly lowers the scattering angle (see Figure 1b), even in the case no relaxation is employed. However, some scattering of parcels still occurs. Employing the BGK-like relaxation (Figure 1c) finally yields a parcel behavior similar to the one observed in the original system with 250-times more particles.

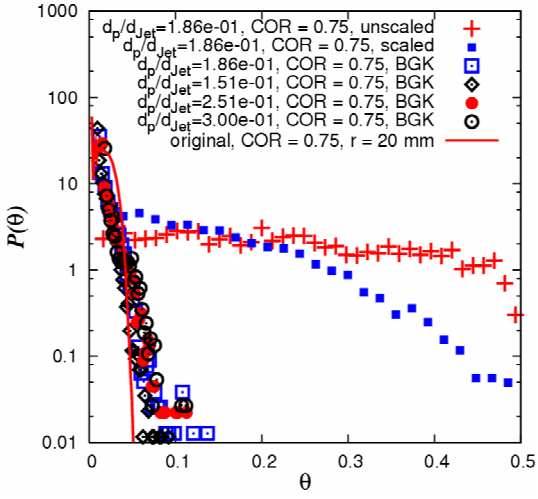

Figure 2: The scattering angle distribution - comparison of the original system (red line), with results using the parcel approach (symbols).

To quantify the effect of the BGK-like relaxation, we compare the distribution of particle scattering angles in Figure 2. Specifically, we plot the number density distribution $P(\theta)$ of the scattering angle θ (i.e., the angle measured between the impact surface and the particle position as illustrated in Figure 1a). To calculate $P(\theta)$, we only consider particles located at a radial distance of R_{sample} = 63.5 ± 2.5 mm from the origin, as per Cheng et

al., 2007; for the original system, though, we set R_{sample} = 20 ± 2.5 mm, since we were unable to simulate the full system. As can be seen from Figure 2, the unscaled and scaled systems give a wide distribution of scattering angles, with scattering half angles θ_{half} (defined as $\int_0^{\theta_{half}} P(\theta)d\theta = 0.5$) of 0.28 and 0.14, respectively. This result is in distinct contrast to the very narrow distribution of the original system (shown by the red line in Figure 2). However, when we employ the relaxation model, all simulations using a larger parcel diameter (see the symbols for different values of d_p/d_{jet} in Figure 2) agree reasonably well with behavior of the original system. The improved agreement of the BGK cases indicates the importance of the relaxation model in replicating the behavior of the much smaller particles within a parcel.

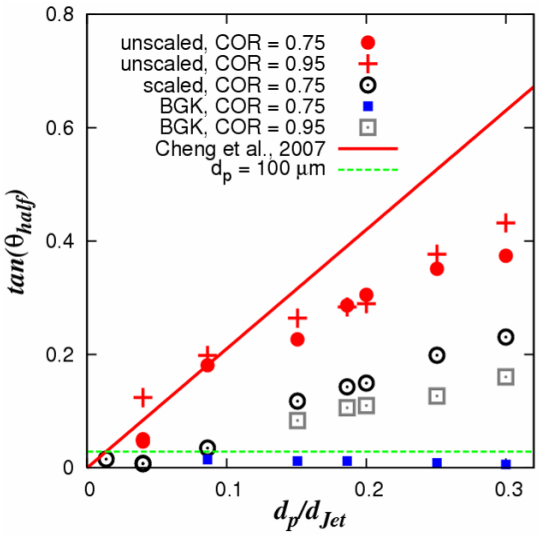

Figure 3: The scattering half angle θ_{half} as a function of dimensionless parcel size (symbols represent simulation results, lines are theoretical predictions).

In Figure 3 we show a summary of our results for the granular jet for various scalings, expressed as d_p/d_{jet}. Clearly, when the system is unscaled (filled circles and crosses), the parcels behave like large particles. In this systems the scattering half angle is close to the correlation established by Cheng et al., 2007, and given in Eqn. 21. For the unscaled system we find that the coefficient of restitution has no significant effect at large dimensionless parcel diameters. Only for the smallest system studied (i.e., d_p/d_{jet} = 0.04) there is a large relative difference for our results involving e_p = 0.75 and e_p = 0.95. The cause for this behavior is unclear, as previous computational studies (e.g., that of Huang et al., 2010) could not afford to simulate that large systems (the simulations for d_p/d_{jet} = 0.04 required us to track 0.97 million particles) and the experiments of Cheng et al., 2007, only included particles that had a coefficient of restitution equal to 0.75.

The scaled system using the BGK-like relaxation model (blue filled squares in Figure 3) shows a more realistic behavior, as we obtained the small scattering angles typical for a system made up by particles of 100 µm (the scattering angle for 100 µm particles as expected from Eqn. 21 is shown as green dashed line Figure 3). Our simulation results for the original system are indicated by the leftmost black circle at d_p/d_{jet} = 0.0137. These simulations involved already 2.7 million particles in a domain half the size as the one used for the other cases. Our results when using the relaxation model (blue filled squares in Figure 3) are somewhat below the expected results from Eqn. 21, as well as our simulations of the original system. This behavior is also visible in Figure 2, where the simulation results using the BGK relaxation do not match perfectly with the original system (red line in Figure 2). It seems that the chosen expression for the relaxation time slightly over-predicts the collision frequency, even though we already subtract the collision frequency between parcels. More work, and possibly a more suitable model, is required to explain this difference, and to make the scattering angles in both systems collapse. Another explanation could be that the switch off particle volume fraction of $\phi_{p,off}$ = 0.60 in our simulations is somewhat too high. Indeed, simulations with lower values for $\phi_{p,off}$ showed that such a parameter adjustment could be used to improve the collapse. However, there is no rationale for choosing a different value for $\phi_{p,off}$, and hence we suggest to first improve the collision frequency model, rather than to perform a parameter fit.

Simple Shear

We performed simple shear flow simulations using a cubic box of particles. Lees-Edwards boundary conditions (LEBCs, Lees and Edwards, 1972) were employed on two sides of the box, whereas on the other four sides periodic boundaries were set. The LEBCs impose a steady shear motion on the particles. Stresses, fabric tensors, velocities, as well as particle rotation rates were recorded during the simulation, and then averaged over the box. Stresses were probed by calculating the contact and streaming stress tensor for each particle, and then summing up the contributions from each particle. A similar procedure was employed for the fabric tensor (results not shown). Both procedures (i.e., for the stress and the fabric) follow the work of Latzel et al., 2000. The granular temperature in the system was estimated by calculating the velocity fluctuation tensor $\underline{\underline{\mathbf{v}}}^2_{p,fluct}$, and then setting

$$T = tr\left(\underline{\underline{\mathbf{v}}}^2_{p,fluct}\right)\Big/3 . \qquad (22)$$

The velocity fluctuations were calculated from the instantaneous particle velocity and the local average velocity. The latter was calculated under the assumption of a linear velocity profile.

Similar to the granular jet, we performed shear flow simulations in (i) an unscaled system (i.e., the interaction parameters for the contact model were not changed with parcel size); (ii) a scaled system (scaling based on Eqn. 10), but without relaxation model; as well as (iii) a scaled system with relaxation model. For our simulations we used the same particle interaction parameters as shown in Table 1, except for μ_{roll}, which was set to zero. Simulations were performed with ϕ_P =

0.55, e_p = 0.75, and the shear rate was chosen such that $\gamma^* = \gamma \cdot d_{prim} \Big/ \sqrt{k/(\rho_p \cdot d_{prim})} = 10^{-4}$ was constant. Systems with different parcel sizes where investigated by holding the box size (0.015 m) and the primary particle diameter (d_{prim} = 100 µm) constant, and grouping between 4 and 8192 particles into one parcel. Also, a limited number of simulations were performed with ϕ_P = 0.62 to show the system behavior in the quasi-static flow regime. Each of these simulations involved approximately 4,000 parcels in a box of variable size to investigate the effect of the parcels size.

Granular Temperature

Already previous work (Benyahia and Galvin, 2010) showed that the granular temperature in a wall-bounded shear flow dramatically increases with parcel size. This finding is expected, since a simple calculation based on the kinetic theory of granular flow would predict that (see, e.g., Sangani et al., 1996):

$$\frac{T}{(\gamma \cdot d_p)^2} = \frac{1+\pi/12 \cdot [1+5/(8 \cdot \phi_p \cdot g_0)]^2}{15 \cdot (1-e_p)} \qquad (23)$$

Here g_0 is the radial distribution function at contact, for which we use the expression in Eqn. 15. Thus, by just scaling the particle diameter, and performing a naive DEM-based simulation leads to a significant overestimation of the granular temperature in the system.

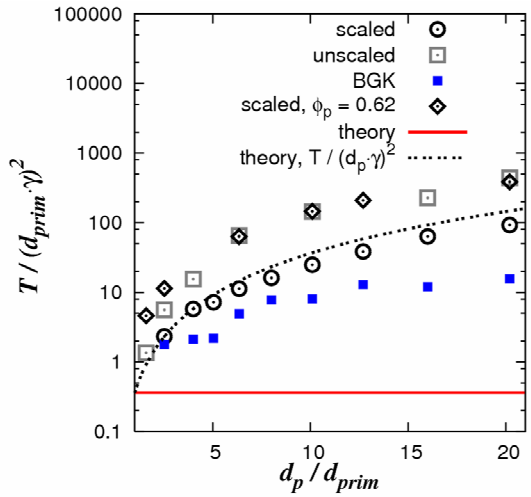

Figure 4: Granular temperature scaled by the velocity fluctuation in the original system $(d_{prim} \cdot \gamma)^2$ (symbols represent simulation results, lines are theoretical predictions, ϕ_P = 0.55 unless otherwise stated).

The results for the granular temperature (made dimensionless with the shear rate and the primary particle diameter d_{prim}) are shown in Figure 4. The red bold line represents the expected granular temperature of the original system for ϕ_P = 0.55 estimated from Eqn. 23, which should remain constant when using the relaxation model. Also, we have included a line representing the theoretical prediction using Eqn. 23 for the increase in granular temperature in the simulations without relaxation model (i.e., the scaled and unscaled system should behave like a system consisting of large particles, and the granular temperature should increase proportional to $(d_p/d_{prim})^2$). Clearly, the results for the scaled system and ϕ_P = 0.55 agree reasonably well with the theory of Sangani et al., 1996, which slightly overpredicts the granular temperature. The unscaled system, as well as the scaled system with ϕ_P = 0.62 shows a higher granular temperature, but the same principal trend as the theoretical prediction of Sangani et al., 1996. This is because the unscaled system represents a case with a higher coefficient of restitution - this increase can be easily understood by inspection of Eqn. 23. The scaled system with ϕ_P = 0.62 is in the quasi-static regime, for which the theory of Sangani et al., 1996, is no longer applicable.

The simulations using the BGK-like relaxation in Figure 4 show a lower granular temperature, i.e., the system behavior is closer to the theoretical prediction of the original system (bold red line). Still the granular temperature is significantly overpredicted using the relaxation model given by Eqns. 14 and 18. Thus, the relaxation to the local mean velocity is too week to dampen the velocity fluctuations of the parcels. Also, the scaled granular temperature increases with parcel size, indicating that the dependency of the current relaxation model on the parcel size is too weak.

Stresses

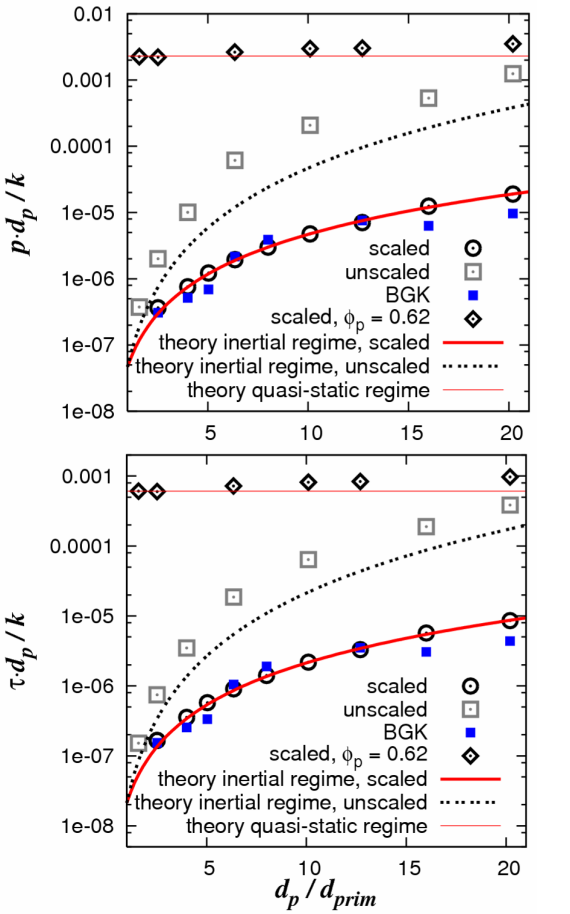

Figure 5: Pressure (top) and shear stress (bottom) for different parcel diameters and filter sizes in a scaled and unscaled system, as well as a in a system with BGK-like relaxation (symbols represent simulation results, lines are theoretical predictions, ϕ_P = 0.55 unless otherwise stated).

The results for the sum of contact and streaming stresses are shown in Figure 5. Here we have defined the pressure as $p = (\sigma_{xx} + \sigma_{yy} + \sigma_{zz}) / 3$, and the shear stress τ is the stress component pointing in the shearing direction and acting on the surface normal to the gradient direction (the other shear stress components are much smaller).

As can be seen from Figure 5, with increasing parcel size both pressure and shear stress dramatically increase for the systems with $\phi_P = 0.55$. This is explained with the fact that these systems correspond to a system with a higher dimensionless shear rate $\gamma^{*'}$, in case we define this dimensionless shear rate with $\gamma^{*'} = \gamma \cdot d_p \Big/ \sqrt{k/\left(\rho_s \cdot d_p\right)}$, i.e., we use the parcel diameter instead of the primary particle diameter. Thus, $\gamma^{*'}$ increases with $(d_p/d_{prim})^{3/2}$ in the unscaled system, and with (d_p/d_{prim}) in the scaled system since our scaling is based on k/d_p = const. As our simulations were performed with $\mu_{PP} = 0.1$, and $\gamma^{*'} < 10^{-2}$, the systems with $\phi_p = 0.55$ were in the inertial regime, and the systems with $\phi_p = 0.62$ were in the quasi-static regime (for an exact regime definition refer to Chialvo et al., 2011). Previous studies, and simple theory tells us that pressure and shear stress scale with the dimensionless shear rate squared in the inertial regime (at constant volume fraction and friction coefficient). In the quasi-static regime the stresses are expected to remain constant, and only a moderate increase for $\gamma^{*'} > 10^{-3}$ (which corresponds to $d_p/d_{prim} > 10$ in our scaled system) is anticipated due to a regime transition into an intermediate flow regime (see the findings of Chialvo et al., 2011). We have included lines showing the expected trends for the stresses in the quasi-static and inertial flow regime in Figure 5 (see the red solid lines).

As can be seen, the simulation results for the scaled system agree well with the expected scalings in the inertial and quasi-static regime. For the latter regime our simulation results for the stresses (black diamonds in Figure 5) slightly increase with parcel size above $d_p/d_{prim} = 10$ due to the transition to an intermediate flow regime. This increase has also been observed by Chialvo et al., 2011, for flows at different dimensionless shear rates.

Also the results for the unscaled system with $\phi_p = 0.55$ follow the theoretical predictions for flow in the inertial flow regime; however, they show somewhat higher stresses. This is explained by the fact that for the unscaled system also the coefficient of restitution increases with parcel size, which results in higher granular temperature and stresses.

In case the BGK-like relaxation is applied, the sum of contact and streaming stress stays nearly unaffected (see the filled blue boxes in Figure 5), and only for $d_p/d_{prim} > 15$ a rather small drop in the stresses is observed. Thus, even in case we perform a BGK-like relaxation, the stresses do not significantly change compared to a scaled system.

CONCLUSION

Even though parcel-based approaches have been in use for more than fifteen years since the pioneering work of Andrews and O'Rourke, 1996, there is still a strong need to analyze the basic features of this simulation approach. Recent literature highlights this need (see the work of Benyahia and Galvin, 2010; Benyahia and Sundaresan, 2011).

In this work we performed a relaxation of parcel velocities to a local mean velocity to account for collisions of particles making up the parcels. We claim that such a relaxation is necessary in any DEM-based simulation that uses bigger (pseudo) particles, and has the ambition to model the original system consisting of a much higher number of primary particles. Even in cases where a proper scaling of particle interaction parameters is performed (i.e., a scaling like the one proposed by Bierwisch et al., 2009, or the one presented in this work for the linear spring-dashpot model), a relaxation seems necessary. Thus, our simulations involving the relaxation model gave a nearly parcel-sized independent behavior for a granular jet impinging on a planar surface, while simulations without relaxation did not.

The challenge for parcel-based methods is to correctly compute the collision rate, the granular temperature and the inter-parcel stress in a dilute to moderately dense region. Our simulations for a simple shear flow in the inertial regime agree with the kinetic theory of granular flow that predicts a massive increase in granular temperature and stress with parcel size when no relaxation is used. For the stress this is explained with the higher dimensionless shear rate when parcels are used, i.e., the shear rate increases with $(d_p/d_{prim})^{3/2}$ in an unscaled system, and with d_p/d_{prim} in a system with scaled interaction parameters to yield identical behavior in quasi-static granular flow. Thus, there is no easy way of scaling parcel interaction parameters to yield identical flow behavior in the inertial flow regime. For the quasi-static flow regime, however, scaling is less problematic and we observe a nearly constant stress in our shear flow simulations. Only the transition to an intermediate flow regime, as defined by Chialvo et al., 2011, will lead to an increase in the stresses in a correctly scaled system.

For simple shear flow in the inertial regime the use of the relaxation model based on O'Rourke and Snider, 2010, used in a slightly modified form in our work, leads to a granular temperature for the parcel-based approach closer to the original system, but this is not true for the stress. It is still unclear how one can obtain an identical stress for flows in the inertial regime when using a parcel-based approach. Clearly, more work is required, especially in connection with the relaxation model, which is subject of ongoing work.

ACKNOWLEDGEMENT

We thank Sebastian Chialvo for reviewing the manuscript. SR acknowledges the financial support of the Austrian Science Foundation and Princeton University through the Erwin-Schrödinger fellowship J-3072.

APPENDIX

List of animation files:

(A1) "1000k_boxLEBC_PrincetonLogoMix.avi" (simple shear of 10^6 particles in a box with Lees-Edwards boundary conditions)

REFERENCES

ANDREWS, M.J. and O'ROURKE, P.J., (1996), "The multiphase particle-in-cell (MP-PIC) method for dense particulate flows", *International Journal of Multiphase Flow*, **22**, 379-402.

BENYAHIA, S. and GALVIN, J.E., (2010), "Estimation of Numerical Errors Related to Some Basic Assumptions in Discrete Particle Methods", *Industrial & Engineering Chemistry Research*, **49**, 10588-10605.

BENYAHIA, S. and SUNDARESAN, S., (2011), "Do We Need Sub-grid Scale Corrections for Both Continuum and Discrete Gas-Particle Flow Models", *(Submitted for Publication)*.

BIERWISCH, C., KRAFT, T., RIEDEL, H., and MOSELER, M., (2009), "Three-dimensional discrete element models for the granular statics and dynamics of powders in cavity filling", *Journal of the Mechanics and Physics of Solids*, **57**, 10-31.

CHENG, X., VARAS, G., CITRON, D., JAEGER, H.M., and NAGEL, S.R., (2007), "Collective behavior in a granular jet: Emergence of a liquid with zero surface tension", *Physical Review Letters*, **99**, 188001-1-188001-4.

CHIALVO, S., SUN, J., and SUNDARESAN, S., (2010), "Rheology of simple shear flows of dense granular assemblies in different regimes", APS DFD Meeting, Long Beach, California, American Physical Society.

CHIALVO, S., SUN, J., and SUNDARESAN, S., (2011), "Bridging the rheology of granular flows in three regimes", *(Submitted for Publication)*.

CLEARY, P.W., (2009), "Industrial particle flow modelling using discrete element method", *Engineering Computations*, **26**, 698-743.

DARABI, P., POUGATCH, K., SALCUDEAN, M., and GRECOV, D., (2010), "Agglomeration of Bitumen-Coated Coke Particles in Fluid Cokers", *International Journal of Chemical Reactor Engineering*, **8**, A122.

HUANG, Y.J., CHAN, C.K., and ZAMANKHAN, P., (2010), "Granular jet impingement on a fixed target", *Physical Review e*, **82**, 031307-1-031307-8.

JENKINS, J.T. and BERZI, D., (2010), "Dense inclined flows of inelastic spheres: tests of an extension of kinetic theory", *Granular Matter*, **12**, 151-158.

LATZEL, M., LUDING, S., and HERRMANN, H.J., (2000), "Macroscopic material properties from quasi-static, microscopic simulations of a two-dimensional shear-cell", *Granular Matter*, **2**, 123-135.

LEES, A.W. and EDWARDS, S.F., (1972), "Computer Study of Transport Processes Under Extreme Conditions", *Journal of Physics Part C Solid State Physics*, **5**, 1921-1929.

LINK, J.M., GODLIEB, W., TRIPP, P., DEEN, N.G., HEINRICH, S., KUIPERS, J.A.M., SCHONHERR, M., and PEGLOW, M., (2009), "Comparison of fibre optical measurements and discrete element simulations for the study of granulation in a spout fluidized bed", *Powder Technology*, **189**, 202-217.

LUDING, S., (2008), "Cohesive, frictional powders: contact models for tension", *Granular Matter*, **10**, 235-246.

MOKHTAR, M.A., KUWAGI, K., TAKAMI, T., HIRANO, H., and HORIO, M., (2011), "Validation of the Similar Particle Assembly (SPA) Model for the Fluidization of Geldart's Group A and D Particles", *AIChE Journal (Accepted)*.

O'ROURKE, P.J. and SNIDER, D.M., (2010), "An improved collision damping time for MP-PIC calculations of dense particle flows with applications to polydisperse sedimenting beds and colliding particle jets", *Chemical Engineering Science*, **65**, 6014-6028.

O'ROURKE, P.J., ZHAO, P., and SNIDER, D., (2009), "A model for collisional exchange in gas/liquid/solid fluidized beds", *Chemical Engineering Science*, **64**, 1784-1797.

PATANKAR, N.A. and JOSEPH, D.D., (2001), "Modeling and numerical simulation of particulate flows by the Eulerian-Lagrangian approach", *International Journal of Multiphase Flow*, **27**, 1659-1684.

RADEKE, C. and KHINAST, J.G., (2011), "Wet Mixing of Powders - a Large Scale GPU Implementation", *(in Preparation)*.

RADEKE, C.A., GLASSER, B.J., and KHINAST, J.G., (2010), "Large-scale powder mixer simulations using massively parallel GPU architectures", *Chemical Engineering Science*, **65**, 6435-6442.

RADMANESH, R., CHAN, E., and GRAY, M.R., (2008), "Modeling of mass transfer and thermal cracking during the coking of Athabasca residues", *Chemical Engineering Science*, **63**, 1683-1691.

REDDY, K.A. and KUMARAN, V., (2007), "Applicability of constitutive relations from kinetic theory for dense granular flows", *Physical Review e*, **76**, 061305.

SAKAI, M. and KOSHIZUKA, S., (2009), "Large-scale discrete element modeling in pneumatic conveying", *Chemical Engineering Science*, **64**, 533-539.

SAKAI, M., SHIBATA, K., KAWASAKI, V.M., and KOSHIZUKA, S., (2010), "Numerical Simulation of a Bubbling Fluidized Bed by the Coarse Grain Modeling of DEM (in Japanese)", *Journal of the Society Powder Technology Japan*, **47**, 17-25.

SANGANI, A.S., MO, G.B., TSAO, H.K., and KOCH, D.L., (1996), "Simple shear flows of dense gas-solid suspensions at finite Stokes numbers", *Journal of Fluid Mechanics*, **313**, 309-341.

SILBERT, L.E., GREST, G.S., BREWSTER, R., and LEVINE, A.J., (2007), "Rheology and contact lifetimes in dense granular flows", *Physical Review Letters*, **99**, 068002-1-068002-4.

SNIDER, D.M., (2001), "An incompressible three-dimensional multiphase particle-in-cell model for dense particle flows", *Journal of Computational Physics*, **170**, 523-549.

SNIDER, D.M., (2007), "Three fundamental granular flow experiments and CPFD predictions", *Powder Technology*, **176**, 36-46.

ZHAO, P., O'ROURKE, P.J., and SNIDER, D., (2009), "Three-dimensional simulation of liquid injection, film formation and transport, in fluidized beds", *Particuology*, **7**, 337-346.